

Improved approximation of the Brinkman equation using a lattice Boltzmann method

by

**Nicos S. Martys
Building and Fire Research Laboratory
National Institute of Standards and Technology
Gaithersburg, MD 20899 USA**

Reprinted from *Physics of Fluids*, Vol. 13, No. 6, 1807-1810, June 2001.

NOTE: This paper is a contribution of the National Institute of Standards and Technology and is not subject to copyright.



NIST

National Institute of Standards and Technology
Technology Administration, U.S. Department of Commerce

BRIEF COMMUNICATIONS

The purpose of this Brief Communications section is to present important research results of more limited scope than regular articles appearing in Physics of Fluids. Submission of material of a peripheral or cursory nature is strongly discouraged. Brief Communications cannot exceed four printed pages in length, including space allowed for title, figures, tables, references, and an abstract limited to about 100 words.

Improved approximation of the Brinkman equation using a lattice Boltzmann method

Nicos S. Martys

Building Materials Division, Building and Fire Research Laboratory, National Institute of Standards and Technology, Gaithersburg, Maryland 20899

(Received 19 October 1999; accepted 19 February 2001)

In this Brief Communication, a new approach to generalize the lattice Boltzmann method to produce fluid flow consistent with the Brinkman equation is presented. The method described in this communication both eliminates second order errors in velocity and improves stability over that of a previously proposed lattice Boltzmann-based model. [DOI: 10.1063/1.1368846]

Modeling fluid flow in porous heterogeneous materials with more than one typical pore size¹ (e.g., concrete, microporous rocks, and fractured materials) presents a challenge because it is difficult to simultaneously resolve all the microstructural features of the porous medium that are at different length scales. One possible approach is to divide the porous medium into two regions: (1) the larger pores and (2) homogeneous regions of smaller pores. In the larger pores, the Stokes' equations for incompressible flow hold:

$$\nabla p = \mu \nabla^2 \mathbf{v}, \quad (1)$$

$$\nabla \cdot \mathbf{v} = 0, \quad (2)$$

where p is the pressure, \mathbf{v} is the fluid velocity, and μ is the fluid viscosity. Regions with the smaller pores are treated as a permeable medium and flow is described by Darcy's law:

$$\langle \nabla p \rangle = -\frac{\mu}{k} \langle \mathbf{v} \rangle, \quad (3)$$

where k is the permeability of the porous medium and $\langle \rangle$ denotes the volume average.

The two boundary conditions to be satisfied at the pore/permeable medium interface are continuity of the fluid velocity and the shear stress.² Darcy's law alone is not sufficient to satisfy these boundary conditions. The Brinkman equation³ is a generalization of Darcy's law that facilitates the matching of boundary conditions at an interface between the larger pores and the permeable medium. Brinkman's equation is

$$\langle \nabla p \rangle = -\frac{\mu}{k} \mathbf{v} + \mu_e \nabla^2 \langle \mathbf{v} \rangle, \quad (4)$$

where \mathbf{v} is the fluid velocity, μ is the fluid viscosity, and μ_e is an effective viscosity parameter. The so-called effective viscosity should not be thought of as the viscosity of the fluid

but only a parameter that allows for matching of the shear stress boundary condition across the free-fluid/porous medium interface. That is, $(\mu d\langle v \rangle / dy)(y=0^+) = \mu_e d\langle v \rangle / dy(y=0^-)$, where $y=0$ specifies the location of the interface. The + and - refer to regions in the free-fluid and porous medium, respectively.

Although the Brinkman equation is semiempirical in nature it has been validated by a detailed numerical solution of the Stokes' equations in regions near the interface between dissimilar regions.⁴ Numerical solution of the Brinkman equation by more traditional computational methods (e.g., finite difference and finite element) is certainly possible. However, a recent lattice Boltzmann (LB) based model by Spaid and Phelan⁵ (henceforth denoted as model A) has proven to be a simple and computationally efficient method to numerically approximate fluid flow described by the Brinkman equation. While model A is capable of describing the more general case of $\mu_e / \mu \neq 1$, its treatment has always assumed $\mu_e / \mu = 1$ in the absence of any definitive knowledge about this ratio. However, theoretical studies⁶ and numerical simulations⁴ have demonstrated that this limiting case is only true when the porosity, $\phi \rightarrow 1$ and that in reality μ_e / μ increases with solid fraction^{4,6} for similar classes of porous media. For example, when $\phi = 50\%$, it was found that $\mu_e / \mu \approx 4$ for an overlapping sphere model of porous media.⁴ Indeed, μ_e / μ appeared to be independent of how the fluid flow was driven indicating that μ_e / μ can be thought of as a material parameter that depends on the pore geometry. Therefore, it is important to consider this more general case when constructing and validating a numerical method to approximate the Brinkman equation.

To produce flow consistent with the Brinkman equation, a dissipative forcing $\mathbf{F} = -\mu \mathbf{v} / k$ was used in model A.⁵ This forcing was incorporated into a LB model, normally used to approximate the Navier–Stokes equations, by introducing a

velocity shift $\Delta \mathbf{v} = \tau \mathbf{F} / n$ (τ is a relaxation parameter and n is the density) in the Boltzmann equilibrium distribution according to the method of Shan and Chen.⁷ However it is well known that this approach will produce errors of order $\tau^2 F^2$ in the pressure tensor.⁸ Such errors can have a significant impact on the fluid dynamics of such systems.

In this Brief Communication I will describe a lattice Boltzmann approach to numerically approximate the Brinkman equation (henceforth called model B) allowing for the case of $\mu_e / \mu \neq 1$. In contrast to model A,⁵ I will describe how to incorporate the dissipative forcing, due to flow in the porous medium, into a *linear* body force term so that the $O(\tau^2 v^2)$ errors are avoided. Results from numerical simulations, validating this approach and providing a comparison to models A and B, will be given.

In the LB method,⁹⁻¹¹ a typical volume element of fluid is described as a collection of particles that are represented in terms of a particle velocity distribution function at each point in space. The particle velocity distribution $n_i(\mathbf{x}, t)$ is the number density of particles at node \mathbf{x} , time t , and velocity \mathbf{e}_i , where ($i = 1, \dots, b$) indicates the velocity direction. The time is counted in discrete time steps, and the fluid particles can collide with each other as they move under applied forces. For this paper the D3Q19 lattice (three dimensional lattice with $b = 19$)^{10,11} will be utilized (the results can be easily generalized to other lattices). The microscopic velocity \mathbf{e}_i equals all permutations of $(\pm 1, \pm 1, 0)$ for $1 \leq i \leq 12$, $(\pm 1, 0, 0)$ for $13 \leq i \leq 18$, and $(0, 0, 0)$ for $i = 19$. The units of \mathbf{e}_i are the lattice constant divided by the time step. Macroscopic quantities such as the density $n(\mathbf{x}, t)$ and the fluid velocity \mathbf{v} are obtained by taking suitable moment sums of $n_i(\mathbf{x}, t)$. Here $n(\mathbf{x}, t) = \sum_i n_i(\mathbf{x}, t)$ and $\mathbf{v}(\mathbf{x}) = \sum_i n_i \mathbf{e}_i / n(\mathbf{x})$. In our units, the molecular mass m equals 1.

The time evolution of the particle velocity distribution function satisfies the following LB equation:

$$n_i(\mathbf{x} + \mathbf{e}_i, t + 1) - n_i(\mathbf{x}, t) = \Omega_i(\mathbf{x}, t) - g_i, \quad (5)$$

where Ω_i is the collision operator representing the rate of change of the particle distribution due to collisions and g_i is the body force term. The collision operator can be approximated by a BGK scheme⁹⁻¹¹

$$\Omega_i(\mathbf{x}, t) = -\frac{1}{\tau} [n_i(\mathbf{x}, t) - n_i^{(eq)}(\mathbf{x}, t)], \quad (6)$$

where $n_i^{(eq)}(\mathbf{x}, t)$ is the equilibrium distribution and τ is the relaxation time that controls the rate of approach to equilibrium. The equilibrium distribution may take the following form:^{10,11}

$$n_i^{(eq)}(\mathbf{x}) = t_i n(\mathbf{x}) [1 + 3 \mathbf{e}_i \cdot \mathbf{v} + \frac{3}{2} (3 \mathbf{e}_i \mathbf{e}_i : \mathbf{v} \mathbf{v} - v^2)]. \quad (7)$$

For this model, $t_i = 1/36$ for $1 \leq i \leq 12$, $t_i = 1/18$ for $13 \leq i \leq 18$ and $t_{19} = 1/3$. It has been shown that the above lattice Boltzmann formalism leads to a velocity field that is a solution of the Navier–Stokes equation with the kinematic viscosity $\nu = \frac{1}{3}(\tau - \frac{1}{2})$.^{10,11}

In the continuum Boltzmann equation, the body force term is written $\mathbf{a} \cdot \nabla_e n(\mathbf{x}, e)$, where \mathbf{a} is an acceleration field due to a body force. A representation⁸ of this body force

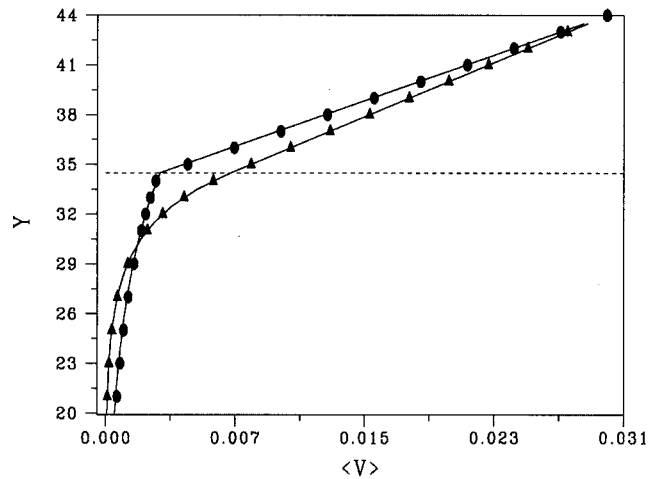


FIG. 1. Velocity field of a sheared system next to a porous medium. The filled triangles and circles represent data from the lattice Boltzmann simulation ($\mu_e / \mu = 1$ and $\mu_e / \mu = 4$, respectively). The solid lines are analytic solutions of the Brinkman equation. The region below the dashed line $y = 34.5$ (in units of lattice spacing) corresponds to the porous medium. The moving wall is at $y = 44$.

term (model B), to second order in Hermite polynomials, in the discrete velocity space of the D3Q19 lattice is

$$g_i = -3 t_i n(\mathbf{x}) [(\mathbf{e}_i - \mathbf{v}) \cdot \mathbf{a} + 3(\mathbf{e}_i \cdot \mathbf{v})(\mathbf{e}_i \cdot \mathbf{a})]. \quad (8)$$

To first order, the body force term is written as $g_i = -3 t_i n(\mathbf{x}) \mathbf{e}_i \cdot \mathbf{a}$. The body force model will henceforth be referred to as model B₁ or B₂ depending on whether the first or second order approximation is used, respectively. To model the momentum loss in the Brinkman equation we take, as in model A,⁵ $n \mathbf{a} = -\mu \mathbf{v} / k$. In addition, the relaxation time to be used in the permeable medium is taken to be $\tau_e = 3(\mu_e / n) + \frac{1}{2}$. In the limit of low Reynolds number, these modifications will recover the Brinkman equation with the option of $\mu_e / \mu \neq 1$. Comparison with model A, where the dissipative forcing is introduced by replacing \mathbf{v} with $\mathbf{v} + \tau \mathbf{F} / n$ in the equilibrium distribution function [Eq. (7)], it is easily seen that this substitution creates errors of order v^2 in the particle distribution function.

To first validate this model, a simple Couette flow geometry was used (see Fig. 1). Starting with a parallel plate geometry, a permeable medium is positioned such that there is a gap between the permeable medium and the upper plate. The upper plate is given a velocity V_w to the right. Analytic solution of the Brinkman equation predicts a linear velocity profile in the gap and an exponentially decaying velocity profile in the porous medium. The rate of decay depends on the value of $\sqrt{\mu_e / \mu}$.^{2,4} In Fig. 1, velocity profiles are compared for the case of $\mu_e / \mu = 4$ and the assumption of $\mu_e / \mu = 1$. The solid line is the analytic solution of the Brinkman solution. Clearly, there is excellent agreement between simulation and theory and there can be a considerable change in the velocity profile when $\mu_e / \mu \neq 1$. In addition, the lattice Boltzmann method also does a reasonably good job capturing the discontinuity of the gradient of the velocity field at the free-fluid/porous medium interface for the case of $\mu_e / \mu = 4$. Note that this is achieved without direct incorpo-

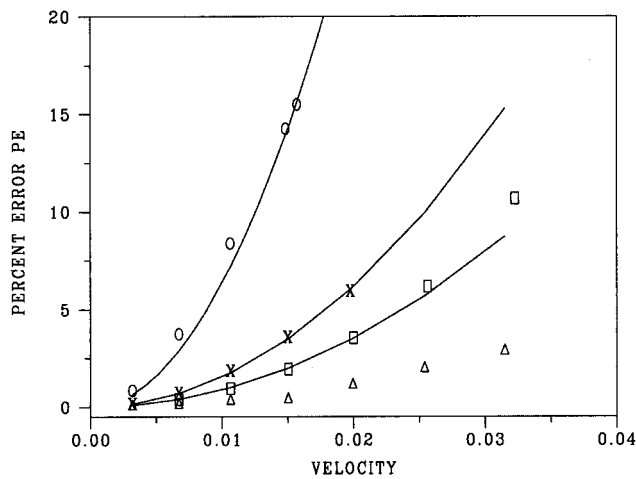


FIG. 2. Percent error in solution vs velocity. Data are shown for the cases of $\tau_e=5$ (\times) and $\tau_e=10$ (circles) for model A, $\tau_e=100$ (triangles) for model B₁ and $\tau_e=5$ for model B₂ (squares). The solid lines correspond to the function av^2 where a is a constant chosen to help guide the eye. Where no data for model B is shown to compare to model A, model A was either unstable or the resulting velocity field oscillated so that no reasonable solution was obtained. Data (not shown) were also obtained for model B₂ with $\tau_e=10$ and found to lie slightly below that shown for $\tau_e=5$ model A.

ration of the stress boundary condition in the simulation model.

While model A should, in principle, account for the case of $\mu_e/\mu \neq 1$ by setting $\tau = \tau_e$, it would still suffer from errors in the particle distribution function, which approximately scales as $\tau_e^2(v/k)^2$. Unfortunately, for many porous media of interest, this error may be large since, in general, as porosity is reduced, μ_e/μ becomes larger as permeability decreases.

As a simple test comparing models A and B, the case of fluid flow in a one dimensional homogeneous porous medium was studied. Here, a pressure drop was applied at opposite ends of the porous medium and the fluid flow was numerically determined throughout the system. For this test case, $k=1/11$ in units of lattice spacing squared. Such a choice of k , ignoring tortuosity effects, corresponds to a porous medium with a typical pore size of an order of lattice spacing as can be seen by noting that the permeability associated with a cylindrical tube is $k=r^2/8$, where r is the tube radius. When using this flow geometry, the solution of Brinkman's equation recovers Darcy's law. Figure 2 compares predictions of flow velocities from models A, B₁, and B₂. Shown is the percent error, (PE) in the solution, defined as $PE=|(V_s - V_t)/V_t|$, where V_s is the fluid velocity determined from the simulation and V_t is the theoretical prediction. It should be pointed out that, for this scenario, the solution of the Brinkman equation will not depend on τ_e since the effective viscosity does not play a role in Darcy flow. From Fig. 2, it can be clearly seen that the error in model A scales as $F^2 \sim \tau_e^2 v^2$ as described earlier. Model B₂ has a weaker dependence on τ_e , roughly scaling as $\tau_e v^2$. In contrast, model B₁ was insensitive to the values of τ_e tested ($1 \leq \tau_e \leq 100$). To better understand these discrepancies, note that a Chapman-Enskog¹² analysis of the lattice Boltzmann BGK model, with body force, shows there is an additional correction to the single particle distribution function

that scales as $\tau_e v F$, i.e., $n_i \approx n^{eq} + n^1 + \dots$, where $n^1 \sim \tau_e v F$ plus the usual viscous corrections.¹² Since, in lattice Boltzmann methods, the pressure tensor is determined from the moment $\Sigma e_i e_j n_i$, it is easy to show that contributions from the body force to this moment sum is zero for model B₁ but produces a correction that scales as $\tau_e v^2$ for model B₂. Careful inspection of model A shows that the same correction ($\sim \tau_e v F$) appears in model A (in addition to the $\tau_e^2 F^2$ correction).

Another interesting point is that model A was found to be numerically unstable at higher velocities shown in Fig. 2. In this velocity regime, errors were found to be approximately 1%–2% for model B₁. Of course it should be pointed out that, due the second order nature of the error obtained using model A, these discrepancies can be significantly reduced by making v smaller or taking τ and τ_e as close as possible to the theoretical stability limit of $\tau = \frac{1}{2}$ for the lattice Boltzmann method. So while model A is still viable for many applications, care must be taken in choosing appropriate parameters for simulations. The two main advantages of model B over model A are: first, one need not be limited to a smaller range of parameter space and second, if the modeler needs to incorporate additional forces in a simulation, a certain obfuscation of the physics can be avoided. Since in model A forces are introduced by shifting the velocity in the equilibrium distribution, additional unphysical terms may arise. For example, if one takes $F = F_1 + F_2 \dots$, where the F_i corresponds to different forces, the F^2 error obtained produces terms like $F_i F_j$ which do not have a physical basis. This is completely avoided if the forces are introduced in a linear fashion as in model B.

In conclusion, a lattice Boltzmann model for numerical solution of the Brinkman equation is presented that can describe the general case of $\mu_e/\mu \neq 1$ and eliminate the second order errors of a previous proposed model.⁵ Indeed, incorporation of the dissipative forcing into a linear body force term extends the validity of this Brinkman approach over a larger range of forcing and effective viscosity. It should also improve numerical accuracy of flow simulations for other applications (Brinkman and non-Brinkman) including: dynamical simulations, linearly driven systems such as that by electromotive forces, and fluid mixtures.

¹F. A. L. Dullien, *Porous Media Fluid Transport and Pore Structure*, 2nd ed. (Academic, San Diego, 1992).

²J. Koplik, H. Levine, and A. Zee, "Viscosity renormalization in the Brinkman equation," *Phys. Fluids* **26**, 2864 (1983).

³H. C. Brinkman, "A calculation of the viscous force exerted by a flowing fluid on a dense swarm of particles," *Appl. Sci. Res., Sect. A* **1**, 27 (1947).

⁴N. Martys, D. P. Bentz, and E. J. Garboczi, "Computer simulation study of the effective viscosity in Brinkman's equation," *Phys. Fluids* **6**, 1434 (1994).

⁵M. A. A. Spaid and F. R. Phelan, "Lattice Boltzmann methods for modeling microscale flow in fibrous porous media," *Phys. Fluids* **9**, 2468 (1997).

⁶S. Kim and W. B. Russel, "Modeling of porous media by renormalization of the Stokes equations," *J. Fluid Mech.* **154**, 269 (1985).

⁷X. Shan and H. Chen, "A lattice Boltzmann model for simulating flows with multiple phases and components," *Phys. Rev. E* **47**, 1815 (1993).

⁸N. S. Martys, X. Shan, and H. Chen, "Evaluation of the external force term in the discrete Boltzmann equation," *Phys. Rev. E* **58**, 6855 (1998).

⁹D. H. Rothman and S. Zaleski, "Lattice-gas model of phase separation:

- Interfaces, phase transitions, and multiphase flow," Rev. Mod. Phys. **66**, 1417 (1998), and references within.
- ¹⁰Y. H. Qian, D. d'Humières, and P. Lallemand, "Lattice BGK models for Navier–Stokes equation," Europhys. Lett. **17**, 479 (1992).
- ¹¹H. Chen, S. Y. Chen, and W. H. Matthaeus, "Recovery of the Navier–Stokes equations using a lattice-gas Boltzmann method," Phys. Rev. A **45**, R5339 (1992).
- ¹²R. L. Liboff, *Kinetic Theory*, 2nd ed. (Wiley, New York, 1998).